Journal of Asian Earth Sciences: X 11 (2024) 100169

Contents lists available at ScienceDirect

Journal of Asian Earth Sciences: X

journal homepage: www.sciencedirect.com/journal/journal-of-asian-earth-sciences-x

Shallow-water carbonate facies herald the onset of the Palaeocene-Eocene Thermal Maximum (Hazara basin, Northern Pakistan)

Mubashir Ali [a,b,*], Giovanni Coletti [a], Luca Mariani [a], Andrea Benedetti [c], Muhammad-Jawad Munawar [d], Saif Ur Rehman [d], Pietro Sternai [a], Daniela Basso [a], Elisa Malinverno [a], Khurram Shahzad [e], Suleman Khan [f], Muhammad Awais [g,h], Muhammad Usman [a], Sébastien Castelltort [b], Thierry Adatte [i], Eduardo Garzanti [a]

[a] Department of Earth and Environmental Sciences, Università di Milano-Bicocca, Milano, Italy
[b] Department of Earth Sciences University of Geneva, Geneva, Switzerland
[c] Department of Natural Sciences, Liceo "Isabella d'Este", Tivoli, Italy
[d] Institute of Geology, University of Punjab, Lahore, Pakistan
[e] Institut für Geologie, Universität Hamburg, Hamburg, Germany
[f] Department of Geology, University of Peshawar, Peshawar, Pakistan
[g] Department of Earth, Environmental and Resources Sciences, University of Naples Federico II, Naples, Italy
[h] Department of Geology, University of Swabi, Swabi, Khyber Pakhtunkhwa, Pakistan
[i] Institute of Earth Sciences University of Lausanne, Lausanne, Switzerland

ARTICLE INFO

Keywords:
Palaeocene hyperthermals
Himalayan Neotethys
Climate Change
Carbonate biofacies
Corals
Larger foraminifera

ABSTRACT

We investigate the Palaeocene succession of the Hazara Basin (Northern Pakistan) to better understand the impact of climate change on marine carbonate-producing organisms. These shallow-water carbonates, deposited during the Late Palaeocene, before the onset of the Palaeocene-Eocene Thermal Maximum, were studied using a quantitative approach to highlight changes in the skeletal assemblage. We recognise a decrease in the abundance of colonial corals and green calcareous algae and an increase in larger benthic foraminifera and red calcareous algae from the early Thanetian to the late Thanetian. Increasing temperatures may represent a plausible cause for the decline of the more sensitive colonial corals in favor of the more tolerant larger benthic foraminifera. A similar pattern is observed in most successions deposited along the margins of the Neotethys Ocean, suggesting a connection with the Late Palaeocene environmental changes that heralded the PETM hyperthermal event. Our stratigraphic analysis of the Hazara Basin strata suggests that the biotic turnovers occurred during the Palaeocene – Eocene transition started already before the onset of the Palaeocene Eocene Thermal Maximum as recorded by the geochemical proxies.

1. Introduction

During the Late Palaeocene, large inputs of greenhouse gases into the atmosphere caused perturbations of the carbon-cycle and led to a significant warming of the global climate (Zachos et al., 2008; McInerney and Wing, 2011; Westerhold et al., 2020). Several hyperthermal events are recognised during the Late Palaeocene - Early Eocene interval (Barnet et al., 2019). Among these episodes, the Palaeocene-Eocene Thermal Maximum (PETM) stands out for its intensity (Zachos et al., 2008; Banerjee et al., 2020). The record of these hyperthermal events, and of the overall Late Palaeocene warming, is strongly reflected by the distribution of shallow-water marine carbonate-producing organisms due to their sensitivity to changing climate and the key-role played by biogenic carbonates in the carbon cycle (Stanley and Hardie, 1998; Ridgwell and Zeebe, 2005).

Numerous studies have been conducted to assess shelfal carbonate production across the Cenozoic geological record (e.g., Esteban, 1996; Kiessling et al., 1999, 2002; Halfar and Mutti, 2005; Nebelsick et al., 2005; Bosellini and Perrin, 2008; Johnson et al., 2008; Wilson, 2008; Perrin and Bosellini, 2012; Perrin and Kiessling, 2012; Pomar et al., 2017; Michel et al., 2018; Aguilera et al., 2020; Pomar, 2020; Cornacchia et al., 2021). Several papers highlighted notable changes in the

* Corresponding author.
E-mail address: mubashir.ali@etu.unige.ch (M. Ali).

https://doi.org/10.1016/j.jaesx.2023.100169
Received 8 April 2023; Received in revised form 27 November 2023; Accepted 30 November 2023
Available online 5 December 2023

distribution of marine benthic carbonate producers during the Late Palaeocene – Early Eocene interval, the most significant of which is the decline in both abundance and size of symbiont-bearing colonial-coral bioconstructions (Scheibner and Speijer, 2008; Zamagni et al., 2012; Pomar et al., 2017; Coletti et al., 2022). However, only a limited amount of well exposed shallow marine carbonate successions covering the Upper Palaeocene – Lower Eocene interval have been thoroughly investigated (e.g., Zamagni et al., 2012). Therefore, very few quantitative data are available for tracking the response of marine carbonate producers during Late Palaeocene environmental changes. More quantitative data and research on ancient habitats are needed to improve our capacity to unveil the past, thereby allowing us to better comprehend the present, and foresee the future (Bialik et al., 2023), and this is especially relevant for the Late Palaeocene. Therefore, the aim of the present study is to improve our knowledge on the distribution of carbonate-producing organisms during this crucial time interval by providing a quantitative analysis of the skeletal assemblages of a Thanetian shallow-water carbonate succession exposed in the Hazara Basin of Northern Pakistan. The studied succession accumulated just before the onset of the PETM and comprises facies dominated by both corals and larger benthic foraminifera (LBF), thus documenting the initial response of important types of benthic calcifiers to periods of global warming. A close comparison with correlative carbonate successions from the Himalaya studied with a similar approach (Nicora et al., 1987; Li et al., 2015, 2017, 2020, 2022; Jiang et al., 2021), and with other successions of the eastern and western Neotethys, allowed us to document, on the large scale, the sedimentary response of carbonate systems to climate change just before the final demise of the eastern Neotethys.

2. Geological setting

The Himalayan foreland basin developed since the onset of subduction of the Indian passive continental margin underneath the Asian active margin at middle Palaeocene time (~60 Ma; Hu et al., 2016), and witnessed the final demise of eastern Neotethys during the Early to Middle Eocene (~50 Ma; Garzanti et al., 1987; Najman et al., 2017). The Hazara Basin (Northern Pakistan) is one of the many depocenters formed as a consequence of the convergence and collision between the Indian and Asian plates (Fig. 1). The studied succession is exposed on the western limb of the Hazara-Kashmir syntaxis (Bossart et al., 1988; Critelli and Garzanti, 1994; Najman et al., 2001) and is bounded by two major thrust faults, the Panjal Thrust in the north and the Main Boundary Thrust in the south (DiPietro and Pogue (2004); Ahsan and Chaudhry, 2008) (Fig. 1).

The Neoproterozoic-Cambrian basement of the basin consists of the Hazara Formation slates and phyllites (Butt, 1972), non-conformably overlain by the Jurassic (Hettangian) fluvio-deltaic coal-bearing sandstones and limestones of the Datta Formation (Abbasi et al., 2012). The overlying inner- to outer-ramp carbonates of the Toarcian to Callovian Samana-Suk Formation (Ahsan and Chaudhry, 2008; Shah et al., 2020) are unconformably followed by the Upper Jurassic to Lower Cretaceous glauconitic shales of the Chichali Formation (Ahsan and Chaudhry, 2008; Shah, 2009), overlain in turn by the Lower to Upper Cretaceous glauconitic sandstones, limestones and dolostones of the Lumshiwal

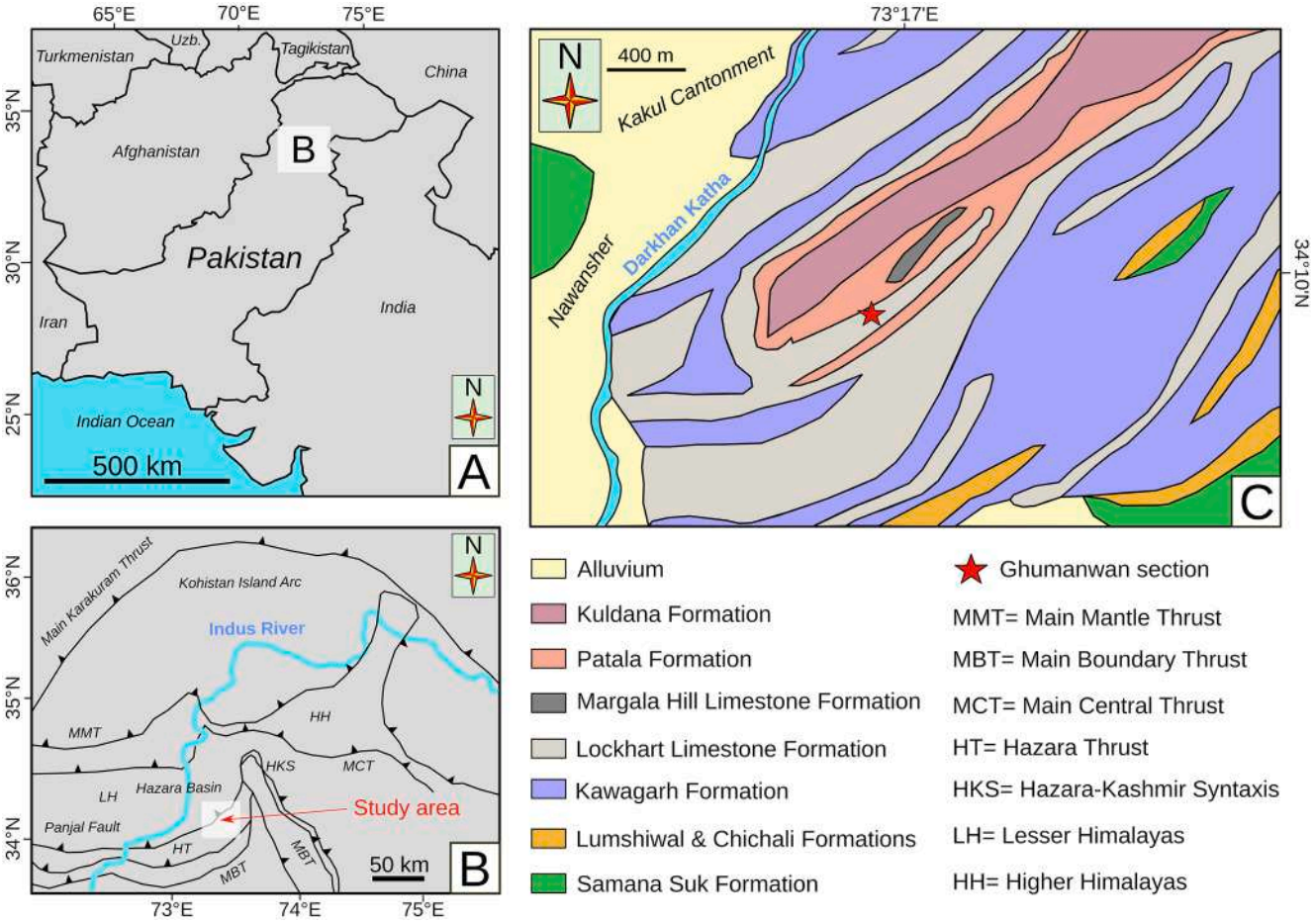

Fig. 1. Study area. A) Location of the study area in Pakistan. B) Schematic tectonic map of the study area showing the main tectonic features (modified from Kazmi and Rana (1982)). C) Simplified geological map of the study area indicating the main formations and the studied section (modified from Afridi, 2010, and Latif, 1970).

Formation. The latter is followed by the Upper Cretaceous deep-water carbonates of the Kawgarh Formation (Ahsan, 2008). The Cretaceous/Cenozoic boundary is marked by bauxite and lateritic palaeosols overlain by the Lower Palaeocene (Danian) Hangu Formation consisting sandstones and coal-rich layers (Ahsan and Chaudhry, 2008; Umar et al., 2015; Saboor et al., 2021). The Hangu Formation is conformably overlain by the shallow-water limestones of the Thanetian Lockhart Limestone (Sameeni et al., 2009), which are followed in turn by the upper Thanetian to lower Ypresian shales of the Patala Formation (Umar et al., 2015). A clear turnover in LBF assemblages is recorded around the Palaeocene-Eocene boundary, when typical Palaeogene LBF's such as *Miscellanea* and *Ranikothalia* were replaced by *Nummulites* and *Alveolina* (Scheibner et al., 2005; Afzal et al., 2011a). The stratigraphic succession of the Hazara Basin continues with the lower Ypresian Margalla Hill Limestone and upper Ypresian nodular limestones of the Chorgali Formation.

The investigated Ghumanwan stratigraphic section (34°10′09.16″ N; 73°16′39.73″ E) is situated in the proximity of the city of Abbottabad (Northern Pakistan). Due to the lack of a detailed geological survey in this part of the Hazara Basin, this section had been previously tentatively correlated with the upper part of the Lockhart Limestone (Fig. 1).

3. Material and methods

The Ghumanwan section was carefully measured, sampled and studied focusing on the distribution of the most relevant fossils (i.e., LBF, corals, and calcareous algae). Palaeontological and petrographic analyses were carried out on 80 thin sections at the Department of Earth and Environmental Sciences (Milano-Bicocca University; Italy). Sixty representative samples of the different lithologies were analysed by powder X-ray diffraction (XRD) at the Geopolis (University of Lausanne; Switzerland). In each of the 29 thin sections prepared from the least recrystallized samples of bioclastic limestones, more than 500 points were counted using a regular spacing of 200 μm (point counting method). Carbonate classification follows Dunham (1962), extended by Embry and Klovan (1971), and refined by Lokier and Al Junaibi (2016). All sufficiently complete and well preserved LBF were identified at the lowest possible taxonomic level and counted together with small porcelaneous, agglutinated, and hyaline benthic and planktic foraminifera (area counting method; Coletti et al., 2021b). LBF identification was performed following mainly Hottinger (2014) for rotaliids, and mainly Leppig (1988), Hottinger (2009), Leppig and Langer (2015), and subordinately other studies (e.g., Di Carlo et al., 2010; Sirel, 2018) for miscellaneids. The taxonomic analysis of LBF was based on a typological approach, whereas miscellaneids were identified at species level by biometric measurements (e.g., Benedetti et al., 2018). The LBF assemblages allowed us to provide biostratigraphic constraints following the biozonal scheme (Shallow Benthic Zones, SBZ) of Serra-Kiel et al. (1998), recently recalibrated for the Palaeocene by Serra-Kiel et al. (2020) and currently adopted also in the eastern Neotethys (e.g., Zhang et al., 2013; Özcan et al., 2015; Kamran et al., 2021; Kakar et al., 2022).

4. Lithology and biofacies

The Ghumanwan section consists of dark-greysh marls (with carbonate content ranging from 20 % to 80 %) overlain by partially recrystallized and slightly deformed limestone beds (carbonate content between 85 % and 95 %) (Figs. 2 and 3). The latter are the focus of this study and can be subdivided into a lower and an upper part. The 43 m-thick lower part mainly consists of very thick beds of massive LBF packstone with patches of colonial-coral framestone (Table 1; Figs. 2 and 3). The 16-m thick upper part, exposed above a 30-m-thick covered interval, also consists of LBF packstone beds and patches of colonial-coral framestone, but it is slightly richer in micritic matrix (Table 1; Figs. 2 and 3). The overall scarce macrofossil content of the limestones is dominated by colonial corals clustered in meters-wide small patches;

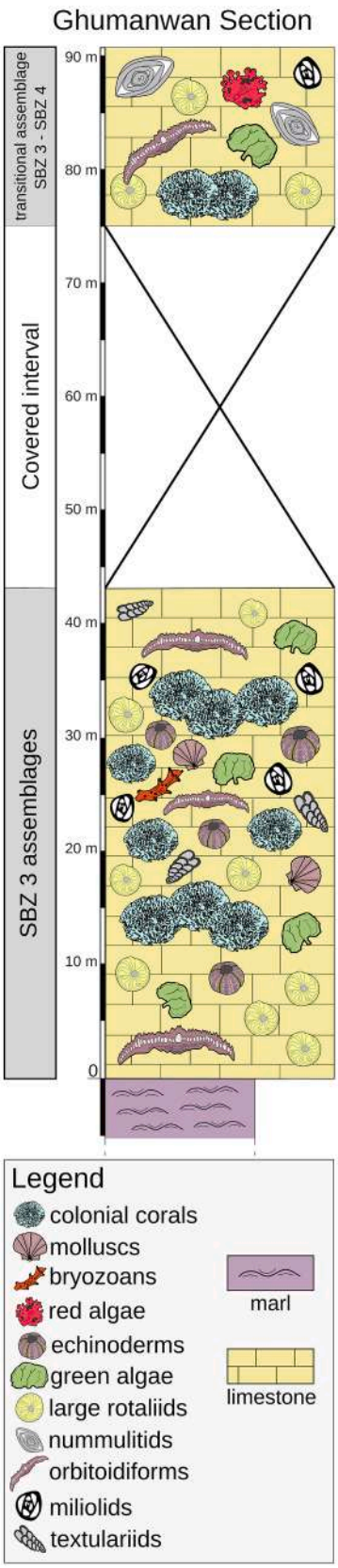

Fig. 2. Investigated interval of the Ghumanwan section.

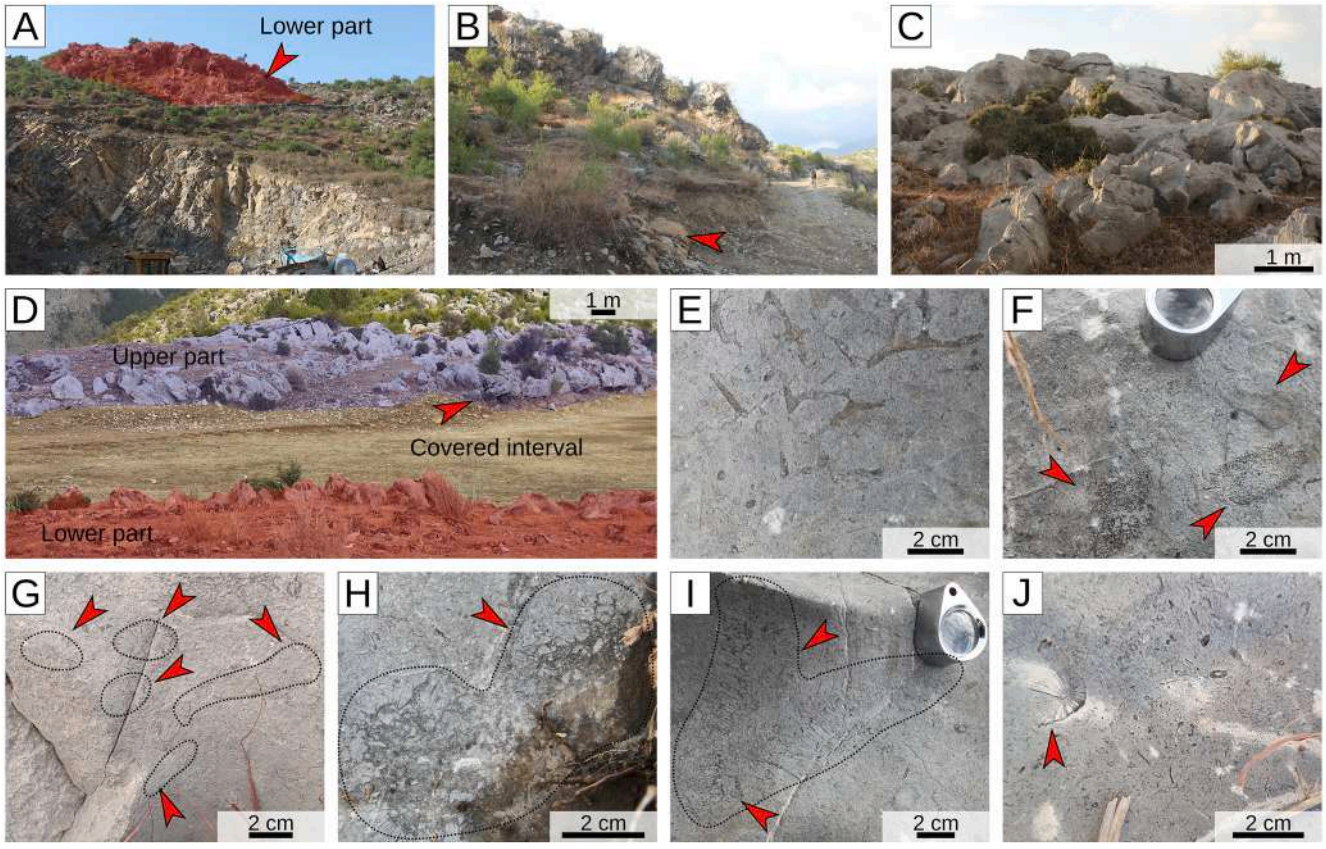

Fig. 3. Ghumanwan Section; the invstigated interval of the section is not overturned and roughly dips towards the North. Lower part: A) panoramic view (red arrowhead = lower part of the investigated interval); B) close-up view (red arrowhead = limestone base); C) topmost strata. Upper part: D) panoramic view (red arrow = basal strata). E) Thin-branched ramose coral colonies. F) Thick-branched ramose coral colonies (red arrowheads = branches). G) Branching corals (red arrowhead = branches). H) Coral colony with a massive morphology (red arrowheads). I) Coral colony with meandroid morphology (red arrowheads). J) Bioclastic material of the limestone (red arrowhead = coral). (For interpretation of the references to colour in this figure legend, the reader is referred to the web version of this article.)

Table 1
Skeletal and foraminiferal assemblages in the Ghumanwan Section. CC = colonial corals; RCA = red calcareous algae; GCA = green calcareous algae; LBF = larger benthic foraminifera; SBF = small benthic foraminifera; EBF = encrusting benthic foraminifera; MOL = molluscs; ECH = echinoderms; BRY = bryozoans.

	SBZ3		Transition SBZ3 to SBZ4	
Lithology	**LBF-packstone**	**coral framestone**	**LBF-packstone**	**coral framestone**
Skeletal assemblage [point counting; %]				
Matrix	57	51.5	64.0	61.5
Clasts	43	48.5	36.0	38.5
Composition of the bioclastic fraction [point counting; %]				
CC	0.6	80.7	0.0	62.2
RCA	0.5	0.0	0.0	20.9
GCA	15.9	1.2	0.8	0.5
LBF	51.9	4.9	75.7	5.4
SBF	27.2	5.1	17.5	2.0
EBF	0.0	0.0	0.0	2.5
MOL	1.6	5.1	1.2	0.7
ECH	2.1	2.0	2.5	4.4
BRY	0.0	0.8	0.0	0.9
Others	0.2	0.1	2.2	0.4
Foraminifera assemblage [area counting; individuals cm^2]				
planktic/benthic ratio	0.014	0.019	0.007	0.025
porcellanaceous/hyaline ratio	0.055	0.060	0.034	0.049
Miscellanea	5.54	0.81	3.52	0.78
Lockhartia	1.99	0.19	2.79	0.11
Nummulitids	0.04	0.07	3.48	0.06
SBF	15.13	4.47	13.84	4.87
Total free-living benthic foraminifera	24.94	6.14	27.18	6.57

rare molluscs were also observed. Coral colonies are poorly preserved and mainly display ramose morphology and, more rarely, massive and meandroid morphologies (Fig. 3E–J).

4.1. Lower limestones

Based on point counting, these packstones are matrix-rich (mostly micrite) and their skeletal assemblage is dominated by LBF with subordinate small benthic foraminifera, green calcareous algae, echinoderms, molluscs, colonial corals, and red calcareous algae (Table 1; Fig. 4). Area counting indicates that, although volumetrically subordinated, small hyaline benthic foraminifera numerically dominate the foraminiferal assemblage together with small miscellaneids (i.e. *Miscellanea yvettae* and *M. juliettae*), and small agglutinated foraminifera. *Lockhartia* and small porcelaneous taxa are also common. *Coskinon* and orbitoidiform taxa are rare. The calcareous algal assemblage is dominated by poorly preserved and heavily recrystallized dasycladacean algae. Small fragments of Peyssonneliales and rare fragments of *Distichoplax biserialis* are also present.

Based on the abundance of the micritic matrix, the meter-wide patches of coral framestone can be considered as intermediate between close-cluster and filled-frame reefs (Table 1; Riding, 2002: Fig. 7). Their skeletal assemblage is dominated by ramose coral colonies associated with benthic foraminifera (mainly small hyaline and small miscellaneids, less diverse and less numerous than in the interbedded packstones), molluscs, echinoderms, rare green calcareous algae, and bryozoans (Table 1; Fig. 5). Although imperfect preservation hindered the identification of coral taxa, some of the best preserved specimens resemble the genus *Bacarella*. The calcareous algal assemblage consists of heavily recrystallized dasycladacean algae, associated with fragments of Peyssonelliales and rare sterile fragments of coralline algae.

The overall foraminiferal assemblage of the lower limestones includes *Coskinon rajkae*, *Elazigina lenticula*, *Lakadongia primitiva*, *Lockhartia haimei*, *L. roeae*, *Miscellanea yvettae*, *M. juliettae*, and *Ranikothalia* sp. (Fig. 7), suggesting a Late Palaeocene age (Serra Kiel et al., 1990; Serra Kiel et al., 2020; Afzal et al., 2011a; Kahsnitz et al., 2016; Papazzoni et al., 2017). The two small species of *Miscellanea* (Fig. 7I–K) suggest the SBZ3 zone (Selandian - early Thanetian), as for similar coeval assemblages from India (Pereira et al., 2022).

4.2. Upper limestones

Based on point counting, these packstones are dominated by LBF, associated with small benthic foraminifera and rare echinoderms, molluscs, green calcareous algae, and very rare ostracods. Based on area counting, the foraminiferal assemblage is dominated by small hyaline foraminifera, nummulitids (mainly *Operculina*), miscellaneids (mainly large morphotypes such as *Miscellanea* cf. *miscella*), *Lockhartia*, and other large hyaline taxa. Small miliolids, agglutinated foraminifera, and orbitoidiforms also present (Table 1; Fig. 7). The scarce calcareous algal assemblage mainly consists of poorly preserved fragments of dasycladacean algae associated with rare sterile coralline algae.

The patches of coral framestone are richer in micrite than those interbedded in the underlying limestone interval, thus displaying a closer affinity with close-cluster reefs (Riding, 2002) (Table 1). Although most coral specimens are poorly preserved, some thin branching

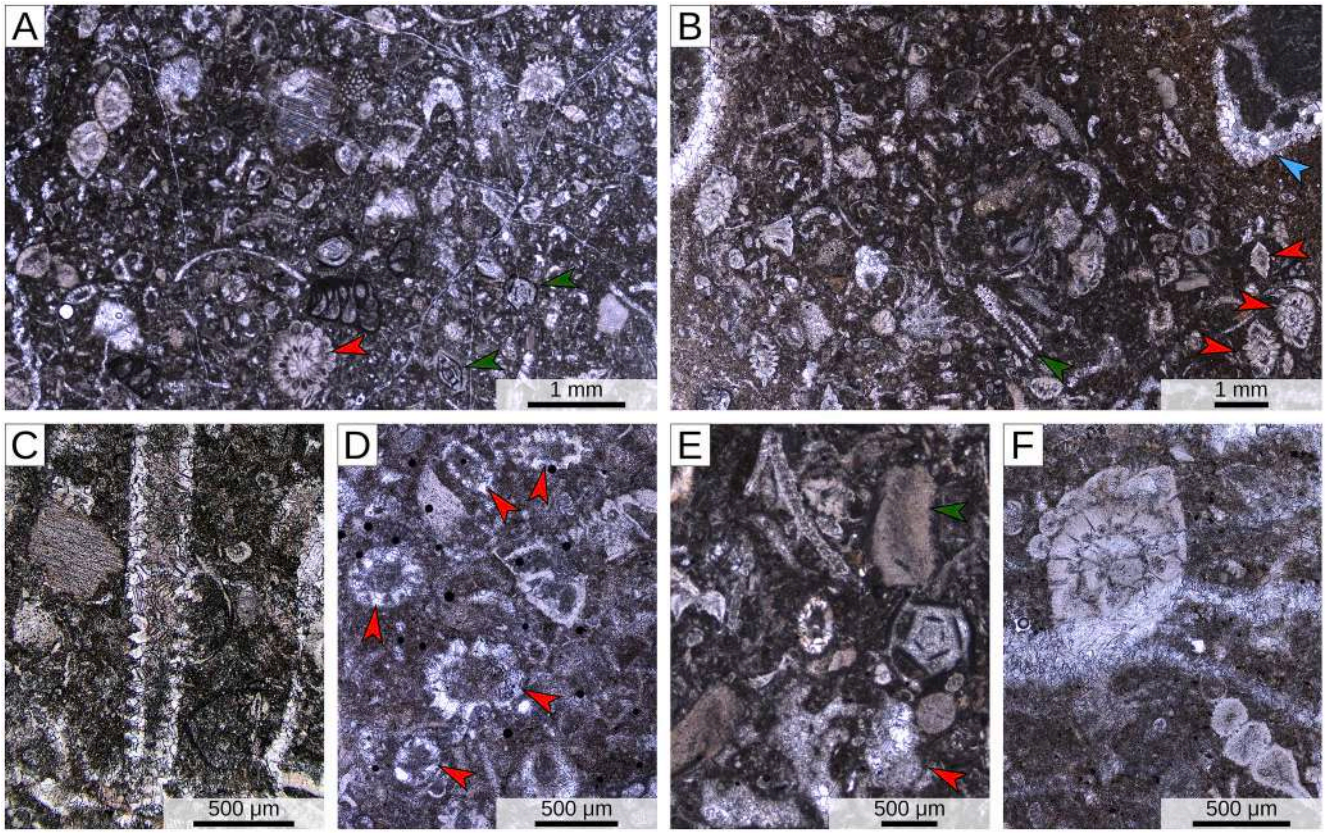

Fig. 4. The lower LBF packstone facies. A, B) Overview (red arrows = small miscellaneid; green arrows = partially recrystallized miliolids in *A* and dasycladacean green calcareous alga in *B*; blue arrow = coral. C) Detail of a dasycladacean alga in axial section. D) Dasycladacean algae in equatorial sections (red arrows). E) Facies detail (red arrow = coral fragment; green arrow = Peyssonneliales red calcareous alga. F) Small miscellaneid. (For interpretation of the references to colour in this figure legend, the reader is referred to the web version of this article.)

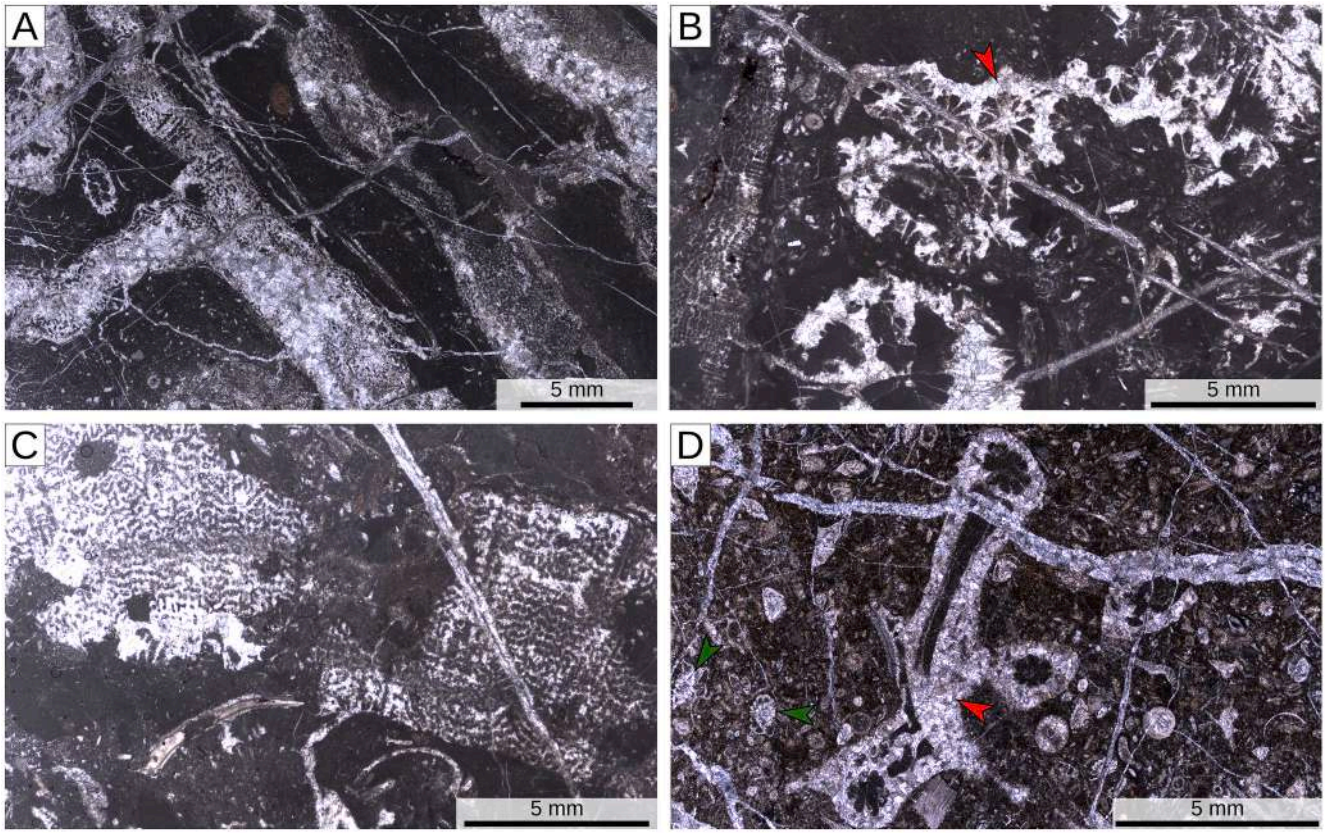

Fig. 5. The lower coral framestone facies. A) Coral colonies. B) Various morphologies of coral colonies (red arrow = possible *Bacarella*). C) Encrusting coral colony. D) Thin-branched coral colony (red arrow) and small miscellaneids (green arrows). (For interpretation of the references to colour in this figure legend, the reader is referred to the web version of this article.)

colonies resemble the genus *Bacarella*. Colonial corals are associated with common red calcareous algae, lesser amounts of larger and small benthic foraminifera (mainly small hyaline taxa and miscellaneids), echinoderms, encrusting foraminifera, and rare bryozoans and molluscs (Table 1; Fig. 8). The calcareous algal assemblage is dominated by Peyssonelliales, associated with common coralline algae (including rare fragments characterised by uniporate conceptacles and thus affine to the order Corallinales), and common *Distichoplax biserialis*.

The overall LBF assemblage of the upper limestones includes *Coskinon* sp., *Daviesina* sp., *Idalina* sp., *Lakadongia* sp., *Lockhartia conditi*, *L. haimei*, *L. roeae*, *L. tipperi*, *Miscellanea yvettae*, *M. juliettae*, *M.* cf. *miscella*, *Orbitosiphon* sp., *Operculina* sp., *Ranikothalia sahnii*, and possibly *Assilina* (Fig. 9), indicating a Thanetian age (Serra Kiel et al., 1998; Serra Kiel et al., 2020; Afzal et al., 2011a; Kahsnitz et al., 2016; Papazzoni et al., 2017). *M. yvettae* and *M. juliettae* are generally considered as markers of SBZ3, but the occurrence of *M. miscella* identifies zone SBZ4 (Hottinger, 2009; Serra-Kiel et al., 2020; Pereira et al., 2022). Although Hottinger (2009) questioned the possibility of distinguishing among the different morphotypes of *M. miscella* at different evolutionary stages, it must be noted that SBZs are mainly Oppelzones based on the concomitant occurrence of phylogenetically unrelated taxa (Pignatti and Papazzoni, 2017) and thus they are not linked to biohorizons or first/last occurrences of single taxa. Because our specimens differ from typical *M. miscella* by having a slightly smaller proloculus and test, they could be considered as basal representatives of the taxon. Gogoi et al. (2009) also documented the co-occurrence of both large and small miscellaneids within a short interval of the Lakadong Limestone (Meghalaya, India). The presence of *M.* cf. *miscella, M. yvettae* and *M. juliettae*, therefore, allows us to consider the upper limestones as transitional between SBZ3 and SBZ4 zones.

5. Discussion

5.1. Palaeoenvironmental evolution

In the studied Ghumanwan succession, LBF packstones are intercalated with patches of coral framestone, pointing to a relatively flat shallow seafloor with flourishing foraminiferal carbonate production interspersed with coral-dominated patch reefs. This type of setting has been envisaged for similar reefs of the Neotethys (e.g., Palaeocene of Lybia, Vršič et al., 2021;Lower Miocene of SE Cyprus; Follows et al., 1996; Coletti et al., 2021a). The presence of red and green calcareous algae, colonial corals, and LBF (Table 1; Figs. 4-9) indicates the photic zone. Small miscellaneids, which are widespread in all the facies of the Ghumanwan section, have been related to reef environments and suggested to be typical of shallow to intermediate water depth (Zamagni et al., 2008; Pereira et al., 2022). A shallow setting is also independently indicated by the scarcity of planktonic foraminifera (Van Der Zwaan et al., 1990). The overall abundance of micrite reflects instead the limited hydrodynamic energy of the environment.

In the coral framestones belonging to the lower limestone interval, calcareous algae are scarce (<2% of the skeletal assemblage) and do not provide much information. The presence of common dasycladacean green calcareous algae in the LBF packstones of the lower interval suggests deposition close or within the upper part of photic zone (euphotic zone sensu Pomar, 2001).

In the coral framestones belonging to the upper limestone interval, the more abundant calcareous algal assemblage (20 % of the total skeletal assemblage) (Table 1) is dominated by Peyssonnelliales and *Distichoplax biserialis* and includes some minor fragments of red algae of the order Corallinales. The latter would suggest a relatively shallow-water setting (Aguirre et al., 2000; Coletti et al., 2018; Coletti and

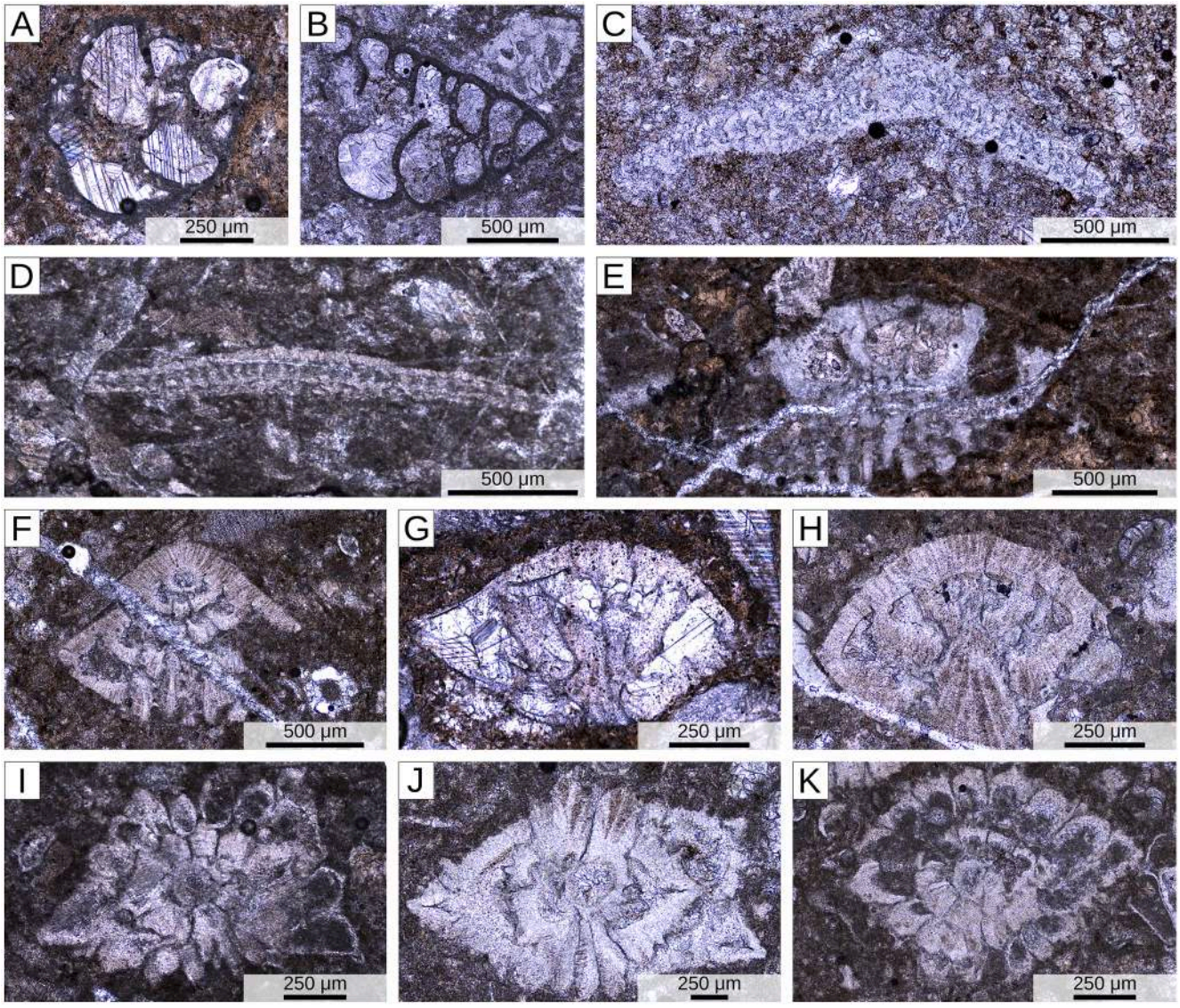

Fig. 6. LBF assemblage of the lower part of Ghumanwan Section. A) *Coskinon raijkae*. B) *Coskinon raijkae* axial section. C) *Lakadongia primitiva*. D) *Lakadongia* sp. E) *Lockhartia haimei*. F) *L. roeae*. G) *Elazigina lenticula*. H) *Kathina* sp. I) *Miscellanea yvettae*, axial section. J) *M. juliettae*, axial section. K) *M. juliettae*, approximately equatorial section.

Basso, 2020). However, the assemblage is dominated by Peyssonnelliales and *Distichoplax biserialis*. Peyssonelliales are a still-living order of red calcareous algae, but the observed taxa of the Ghumanwan section display morphological features very different from their modern relatives (Kato et al., 2006; Pestana et al., 2021), and thus cannot provide us with useful ecological information. *Distichoplax biserialis* has no direct living relatives, but it resembles Corallinales (Sarkar, 2018; Aguirre et al., 2022), thus pointing towards a relatively shallow-water setting. The upper LBF packstones are instead characterised by a scarce calcareous algal assemblage mostly consisting of dasycladacean algae.

The comparison of the assemblages of the lower and upper limestones does not suggest significant changes in water depth throughout the succession (Table 1). More abundant micrite, more nummulitids (e.g., *Operculina*) and less colonial corals and dasycladacean algae may hint to a slightly deeper environment for the upper part of the Ghumanwan section. However, these minor changes are not coupled with other relevant palaeo-bathymetric indicators such as a significant increase in planktic foraminifera or a decrease in miliolids.

5.2. Upper Palaeocene shallow-water carbonates of eastern Neotethys

Coral-framestones display significant differences between the lower (SBZ3) and upper part (SBZ3/SBZ4) of the studied interval of the Ghumanwan section (Table 1; Figs. 4, 5, 7, 8). Micrite and red calcareous algae (in particular *Distichoplax biserialis*) are more abundant in the upper part, where colonial corals become less abundant. LBF-packstones also display differences: micrite and LBF are more abundant in the upper part whereas dasycladacean algae are less abundant.

Similar variations are observed in Upper Palaeocene to Lower Eocene successions of both eastern and western Neotethys. Upper Palaeocene shallow-water carbonates are well represented in northwestern India (Meghalaya area; Jauhri et al., 2006; Sarma and Ghosh 2006; Özcan et al., 2018; Sarkar, 2018, 2020; Sarkar and Narasimha Rao 2018; Pereira et al., 2022), where they are rich in calcareous algae and LBF; colonial corals also occur, but significantly less abundant than in the Hazara Basin (Jauhri et al., 2006; Sarma and Ghosh 2006; Sarkar and Narasimha Rao 2018). Such a scarcity of corals may be related to the excessively high temperatures envisaged by palaeoceanographic models for the eastern Indian part of eastern Neotethys during the late

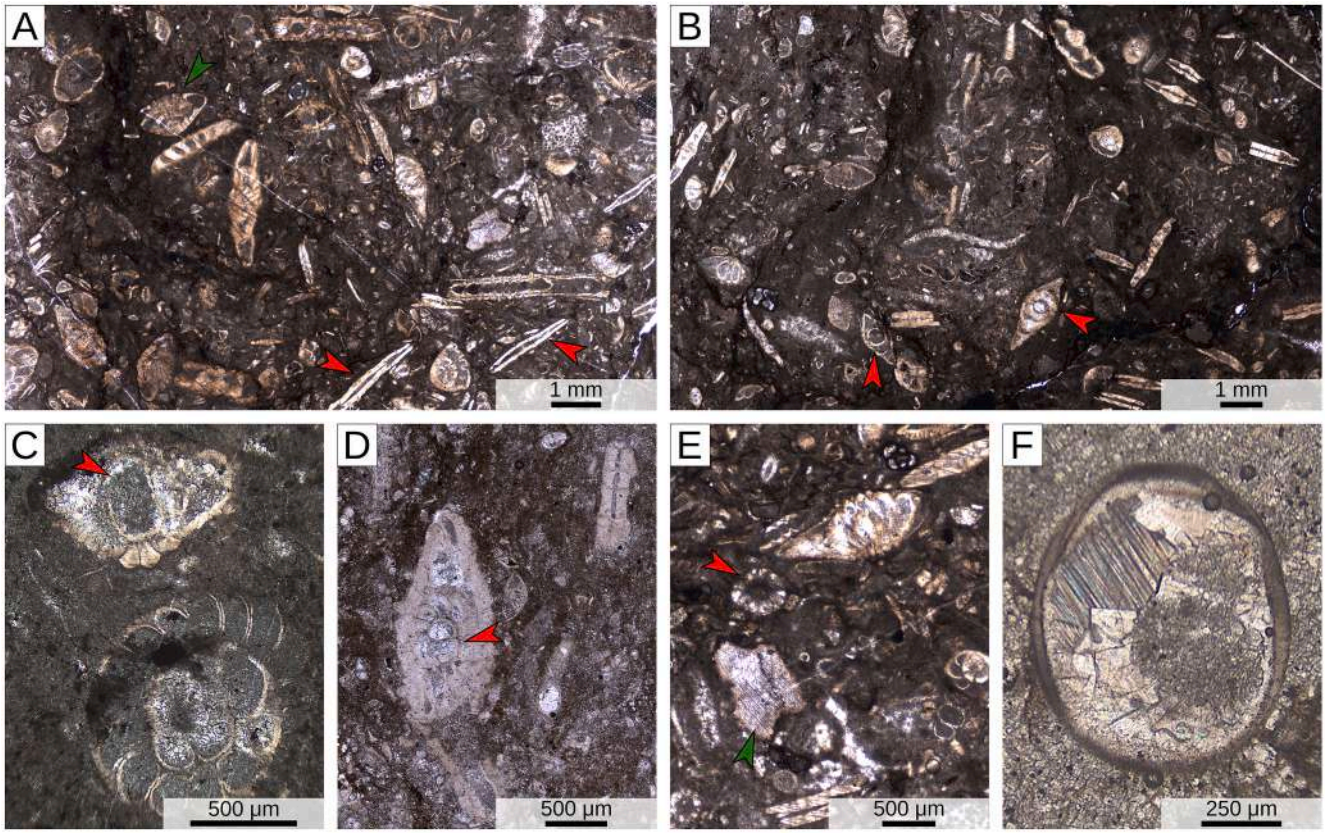

Fig. 7. The upper LBF packstone facies. A, B) Overview (red arrows = *Operculina* in *A*, *Miscellanea* cf. *miscella* in *B*; green arrow = *Lockhartia*. C) *M*. cf. *miscella*, axial and equatorial sections of two different specimens (red arrow = large-sized protoconch). D) Section of *M*. cf. *miscella* crossing the embryo (red arrow). E) Fragment of dasycladacean green alga (red arrow) and echinoderm fragment (green arrow). F) Ostracod. (For interpretation of the references to colour in this figure legend, the reader is referred to the web version of this article.)

Thanetian (Sarkar et al., 2022). Similarly to the Ghumanwan section, a remarkable abundance of *Distichoplax biserialis* is reported in the upper Thanetian (Özcan et al., 2018; Sarkar, 2018; Pereira et al., 2022). In the northeastern Indian area the abundance of this species decreases significantly in the overlying Lower Eocene carbonates (Sarkar, 2018). Common to both Indian area and the Hazara Basin is also the upwards decrease of dasycladacean algae.

In the Tibetan Himalayas, upper Palaeocene shallow-water carbonates are generally dominated by LBF with minor dasycladacean and red calcareous algae; colonial corals rarely occur and no coral-dominated facies is reported (Zhang et al., 2013, 2019; Li et al., 2015, 2017, 2022; Jiang et al., 2021). In the overlying Lower Eocene carbonates, corals, red and green calcareous algae decrease, whereas LBF increase (Li et al., 2015; Li et al., 2017; Li et al., 2020; Li et al., 2022). Similarly to the Ghumanwan Section, a peak in the abundance of *Distichoplax biserialis* is reported in the uppermost Palaeocene (Jiang et al., 2021).

In Upper Palaeocene shallow-water carbonates of Pakistan and Iran, colonial corals are more abundant than in the Himalayas (Afzal et al., 2011b; Bagherpour and Vaziri 2012; Kamran et al., 2021; Shalalvand et al., 2021). Close similarities are observed between the Ghumanwan section and the Taleh Zang Formation in western Iran (Bagherpour and Vaziri 2012; Shalalvand et al., 2021). Here, the lower Thanetian part of the Taleh Zang Formation is dominated by colonial corals and dasycladacean algae (Bagherpour and Vaziri 2012; Shalalvand et al., 2021), whereas the upper Thanetian part of the Taleh Zang Formation records a decrease in colonial corals and an increase in LBF (Bagherpour and Vaziri 2012; Shalalvand et al., 2021). The overlying Lower Eocene shallow-water carbonates are eventually dominated by LBF (Bagherpour and Vaziri 2012; Shalalvand et al., 2021).

Throughout the eastern Neotethys, the quantitative analysis of carbonate facies distribution indicates that colonial corals, red calcareous algae, and green calcareous algae are more common in Palaeocene carbonates than in Eocene carbonates (Coletti et al., 2022).

5.3. Upper Palaeocene shallow-water carbonates of western Neotethys

The Late Palaeocene – Early Eocene decline in colonial corals and the concurrent rise of LBF is documented also in the western Neotethys (Baceta et al., 2005; Scheibner and Speijer, 2008; Zamagni et al., 2008, 2012; Pomar et al., 2017). This is well detailed in the Pyrenees (Table 2). Colonial corals are dominant in Danian strata, decrease progressively through the early and middle Thanetian and sharply in the late Thanetian (Baceta et al., 2005). Similarly to the Ghumanwan section, an increase of the micrite content in coral-dominated bioconstructions can be observed moving from the Lower to the Upper Palaeocene (Table 2). Finally, the peak in the abundance of *Distichoplax biserialis* is once again observed in the uppermost Palaeocene (Li et al., 2022; Aguirre et al., 2022).

An increase in the micrite content of coral-bearing carbonate systems was reported also by Zamagni et al. (2008), while comparing lower and upper Thanetian carbonate systems of Slovenia.

5.4. Response of carbonate producers to Late Palaeocene environmental perturbations

Based on the comparison of carbonate successions from the eastern and western Neotethys, facies changes observed through the Upper Palaeocene in the Ghumanwan section are inferred to herald the more prominent shifts that took place during the Palaeocene–Eocene transition. Although the PETM is considered one of the most relevant

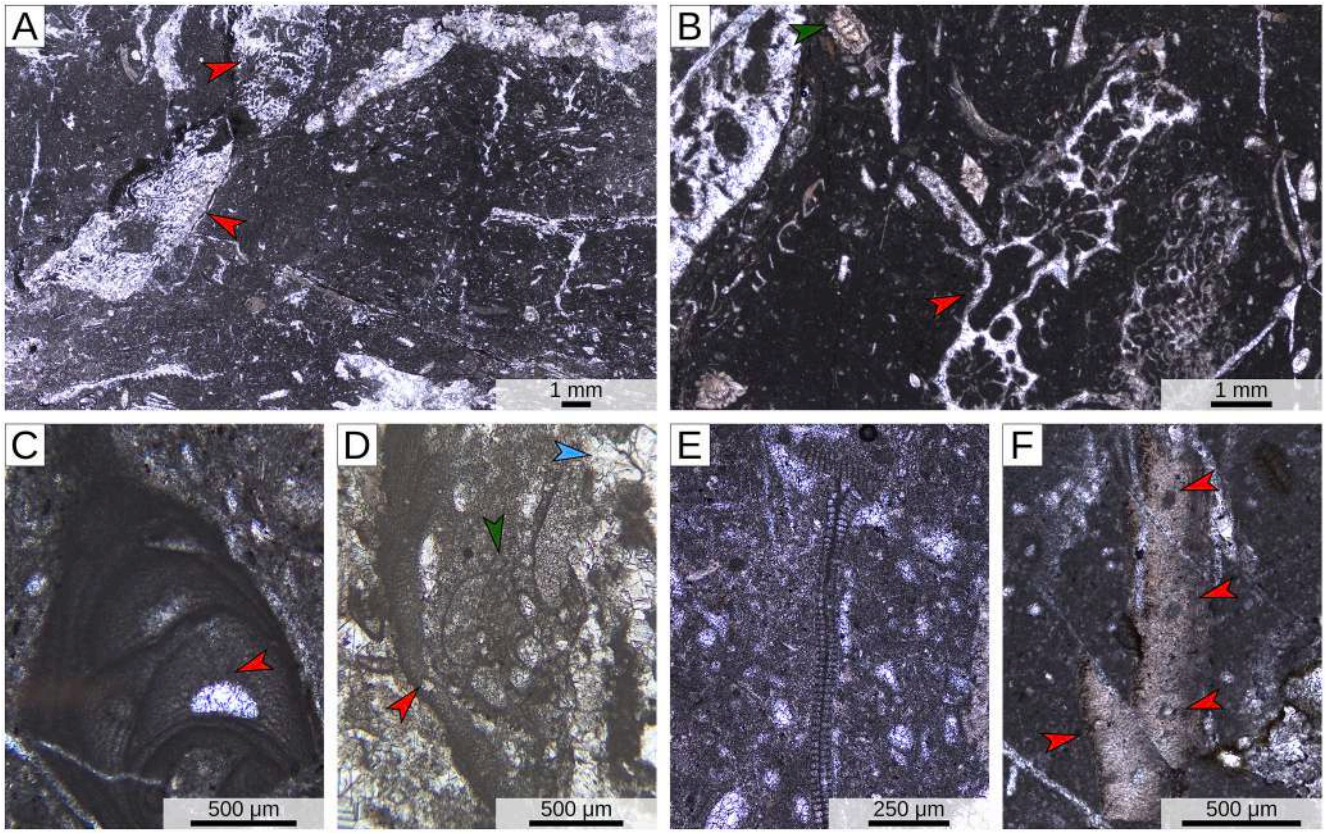

Fig. 8. The upper coral framestone facies. A) Overview (red arrows = colonial corals in *A*, thin-branched coral colony (possibly *Bacarella*) in *B*; green arrow = miscellaneid. C) Coralline alga of the order Corallinales (red arrow = poorly preserved pore of the uniporate conceptacle). D) Encrusting coralline algae (red arrow), encrusting foraminifera (green arrow), and coral (blue arrow). E) *Distichoplax biserialis*. F) Peyssonneliales red calcareous alga (red arrows indicate possible remnants of reproductive structures). (For interpretation of the references to colour in this figure legend, the reader is referred to the web version of this article.)

environmental events of the Cenozoic, the Late Palaeocene warming trend and the Late Palaeocene hyperthermals are also bound to have caused significant changes in marine ecosystems (Long-term Late Palaeocene Perturbation; Bowen et al., 2015; Barnet et al., 2019; Banerjee et al., 2020; Jiang et al., 2022; Tremblin et al., 2022; Vimpere et al., 2023).

The decline of colonial corals as carbonate producers during the Late Palaeocene – Early Eocene time interval has been pointed out by several authors (Baceta et al., 2005; Scheibner and Speijer, 2008; Zamagni et al., 2008, 2012; Pomar et al., 2017), and ascribed by Scheibner and Speijer (2008) and Coletti et al. (2022) to the coeval increase in global temperatures (Bowen et al., 2015; Barnet et al., 2019; Tremblin et al., 2022; Vimpere et al., 2023). Modern colonial corals achieve the highest calcification rates within a narrower temperature range than modern LBF (Crabbe, 2008; Marshall and Clode, 2004; Titelboim et al., 2019). Therefore, the highly adaptable LBF could take competitive advantage from the detrimental effect that high temperatures had on other carbonate producers such as hermatypic corals. Major variations in ocean chemistry were also associated with the PETM (McInerney and Wing, 2011; Jiang et al., 2021; Li et al., 2021), stemming from temperature-induced acceleration of the hydrological cycle, enhanced weathering of continental landmasses, and acidification of oceanic waters caused by the higher CO_2 concentration in the atmosphere (McInerney and Wing, 2011; Sternai et al., 2020; Jiang et al., 2021; Li et al., 2021). These changes in ocean chemistry represent another plausible cause for the decline of corals during the Late Palaeocene – Early Eocene (Zamagni et al., 2012). LBF could have been favored by their greater tolerance to variations in ocean chemistry, and in particular to changes in the supply rate of nutrients (Pomar et al., 2017), and consequently became dominant in the Eocene. Our work shows that the decline of colonial corals as carbonate producers pre-dated the PETM in northern Pakistan, in western Iran, and in the Pyrenees, and thus could be chiefly related to the increase of global temperatures. This is also supported by the distribution of colonial corals along Neotethyan margins during the Late Palaeocene, when they were rare in the warmer eastern Indian region and increasingly common moving westward and northward towards cooler temperatures (Sarkar et al., 2022). Further researches are, however, needed to disentangle the complex relationships among diversity, morphology, colony-size and reef-building potential of corals and global warming events (e.g., Johnson et al., 2008; Bosellini et al., 2022), especially in the case of rapid events like the Palaeogene hyperthermals.

The observed increase in the abundance of red calcareous algae, largely accounted for by the notable increase of *Distichoplax biserialis* from zone SBZ3 to zone SBZ4 followed by its rapid decline (Sarkar, 2018; Li et al., 2021), is harder to explain. Red algae are more tolerant than colonial corals and are known to be able to outcompete colonial corals at tropical latitudes in non-oligotrophic settings (Halfar et al., 2004; Halfar and Mutti, 2005; Coletti et al., 2017; Pomar et al., 2017). The increase in red calcareous algae may thus be ascribed to an increase in nutrient availability caused by Late Palaeocene environmental changes culminating with the PETM. Other explanations are, however, also possible. For instance, coralline algae and other encrusting carbonate producers (e.g., encrusting benthic foraminifera, bryozoans) have been observed to increase in abundance following the deterioration of an environment initially favorable to colonial corals (e.g., upper Oligocene/lower Miocene reefs largely dominated by corals and developed in stable and warm conditions vs. upper Miocene reefs developed in cooler and more stressful conditions and characterized by a variety of encrusting organisms; Bosellini, 2006; Coletti et al., 2019; Coletti et al., 2021a). An increase in water depth can also cause a shift from colonial

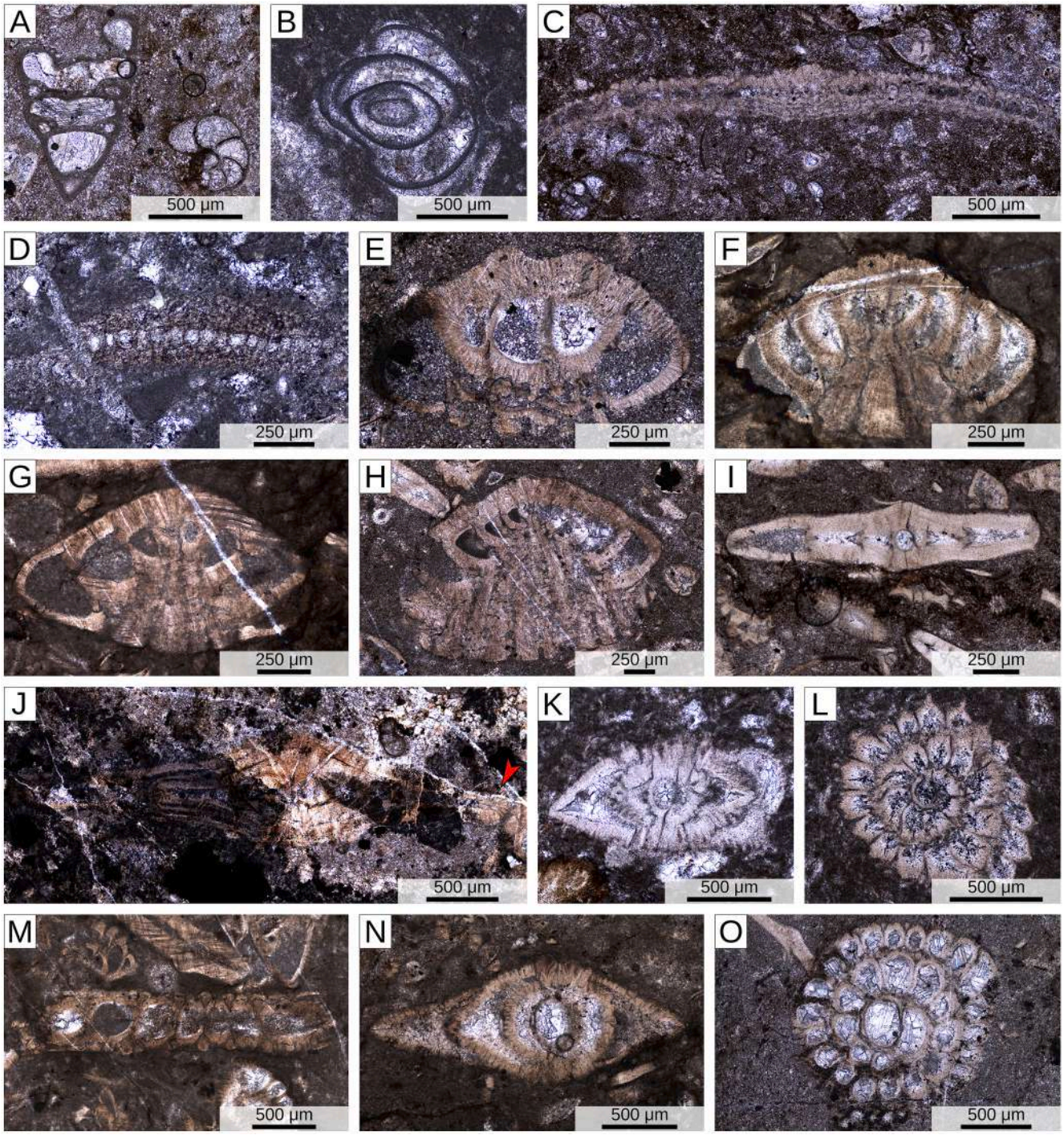

Fig. 9. LBF assemblage of the upper part of Ghumanwan section. A) *Coskinon* sp. B) *Idalina* sp. C) *Lakadongia* sp. D) *Orbitosiphon* sp. E) *Lockhartia haimei*. F) *L. roeae*. G) *L. conditi*. H) *L. tipperi*. I) *Operculina* sp. J) *Ranikothalia sahnii* (red arrow = marginal cord). K) *Miscellanea yvettae*, axial section. L) *M. juliettae*, equatorial section. M) Fragment of *M.* cf. *miscella* in axial section. N) *M.* cf. *miscella*, axial section. O) *M.* cf. *miscella*, equatorial section. (For interpretation of the references to colour in this figure legend, the reader is referred to the web version of this article.)

corals to red calcareous-algal dominated facies (Benisek et al., 2009). These elements suggest that there could be various mechanisms behind an increase in red calcareous algae abundance. Further studies focused on the quantitative distribution of red calcareous algae and *D. biserialis* in particular, might shed light on the effects of Late Palaeocene environmental perturbations on this group of carbonate producers.

Similarly to colonial corals, dasycladacean green calcareous algae also decreased during the Late Palaeocene. Present-day dasycladaceans thrive in restricted and warm lagoonal environments (e.g., Ohba et al., 2017). Therefore, Late Palaeocene warming may not have been the cause of their decline. The coeval decline and extinction of most taxa supposedly able to produce a calcitic skeleton suggest that the decline of Dasycladales may be partly related to a preservation bias during the transition towards modern assemblages entirely constituted of fragile aragonitic taxa (Granier, 2012; Coletti et al., 2022). Once again, quantitative data on the abundance of carbonate-producing organisms (e.g., Bosellini, 1998; Vescogni et al., 2008, 2016; Bosellini et al., 2021; Benedetti and Papazzoni, 2022), generated with a standardized

Table 2
Comparison of coral framestones in the Ghumanwan section and coeval coral reefs of the Pyrenees (Baceta et al., 2005). The relative abundance of diverse components is given using a modified version of the scale proposed by Carey et al. (1995): 0 % = absent; 1 % > very rare > 0 %; 5 % > rare > 1 %; 10 % > scarce > 5 %; 25 % > common > 10 %; 50 % > abundant > 25 %; dominant > 50 %.

Site	Pyrenean Basin Bz-2	Pyrenean Basin Lizarraga pass	Pyrenean Basin Leg-2	Hazara Basin	Hazara Basin
Age	Early-middle Danian ~ 63 Ma	Late Danian ~ 63–61 Ma	Thanetian ~ 59–57 Ma	Thanetian ~ 59 – 57.5 Ma	Late Thanetian ~ 57.5 – 57 Ma
SBZ	SBZ1 - SBZ2	SBZ1 - SBZ2	SBZ3 - SBZ4	SBZ3	SBZ3 to SBZ4
Reference	Baceta et al., 2005	Baceta et al., 2005	Baceta et al., 2005	This work	This work
Characteristics and frame builders					
Matrix	~ 1/2–3/4	~ 1/2–3/4	~ 4/5–2/3	~1/2	~2/3
Grains	~ 1/4–1/2	~ 1/4–1/2	~ 1/5–1/3	~1/2	~1/3
Type of matrix	Sand-sized bioclastic	Sand-sized bioclastic	Micrite	Micrite	Micrite
Non skeletal grains	Absent – very rare	Absent – very rare	Absent	Absent	Absent – very rare
Main frame builders	CC & RCA	CC & RCA	CC & RCA	CC	CC
Secondary frame builders	EBF	EBF	//	//	RCA
Skeletal assemblage					
CC	Abundant	Abundant	Common	Dominant (80.7)	Dominant (62.2)
RCA	Abundant	Abundant	Common	Absent (0.0)	Common (20.9)
GCA	Rare	Rare	Rare	Rare (1.2)	Very-rare (0.5)
LBF	Absent	Absent	Common	Scarce (4.9)	Scarce (5.4)
SBF	Common	Scarce	Common	Scarce (5.1)	Rare (2.0)
EBF	Scarce	Scarce	Scarce	Absent (0.0)	Rare (2.5)
MOL	Rare	Scarce	Scarce	Scarce (5.1)	Very-rare (0.7)
ECH	Rare	Scarce	Rare	Rare (2.0)	Rare (4.4)
BRY	Scarce	Scarce	Common	Very-rare (0.8)	Very-rare (0.9)
Others	Rare	Rare	Rare	Very-rare (0.1)	Very-rare (0.4)
Planktic vs benthic	Entirely benthic	Entirely benthic	Entirely benthic	Entirely benthic	Entirely benthic
Dominant benthic taxa	Small and large hyaline taxa including miscellanids	Small and large hyaline taxa including miscellanids	Large hyaline taxa including nummulitids, mescellanids and orthophragminids and small hyaline taxa	Small hyaline taxa, small agglutinated taxa, miscellanids	Small hyaline taxa, miscellanids

approach, appears to be essential for making more cogent comparisons and improve our knowledge about the response of shallow-water biota to rising temperatures.

6. Conclusions

The so far poorly investigated succession of the Hazara Basin (Pakistan) provides an excellent setting in which to document the initial response of benthic calcifiers to global warming during the Thanetian (Late Palaeocene). The quantitative sedimentological and micro-palaeontological analysis of the Ghumanwan section reveals that this carbonate system underwent significant changes during the Late Palaeocene, just before the onset of the Palaeocene-Eocene Thermal Maximum event (PETM). Colonial corals and green calcareous algae progressively declined, whereas larger benthic foraminifera and red calcareous algae (in particular *Distichoplax biserialis*) became more abundant. The decline of colonial corals and green calcareous algae continued after the PETM, when the more adaptable larger benthic foraminifera emerged as the most significant shelfal carbonate producers. Coral bioconstructions did not become again a widespread feature of carbonate systems until the Oligocene. Similar patterns are recognised in both eastern and western parts of the Neotethys, hinting that the Late Palaeocene changes might be chiefly associated with global warming that culminated in the PETM. While the concurrent decline of symbiont-bearing colonial corals and rise in larger benthic foraminifera can be associated with a reasonably clear and plausible explanation, the distribution pattern of calcareous algae is harder to explain, stressing the need for more quantitative data, generated with a standardized approach, for better constraining the response of shallow-water biota to large scale environmental changes.

CRediT authorship contribution statement

Mubashir Ali: Conceptualization, Investigation, Visualization, Writing – original draft. **Giovanni Coletti:** Conceptualization, Investigation, Visualization, Writing – original draft. **Luca Mariani:** Conceptualization, Investigation, Visualization, Writing – original draft. **Andrea Benedetti:** Investigation, Methodology. **Muhammad-Jawad Munawar:** Investigation, Resources, Writing – review & editing. **Saif Ur Rehman:** Investigation, Resources, Writing – review & editing. **Pietro Sternai:** Conceptualization, Supervision, Writing – review & editing. **Daniela Basso:** Writing – review & editing. **Elisa Malinverno:** Investigation, Methodology, Writing – review & editing. **Khurram Shahzad:** Writing – review & editing. **Suleman Khan:** Writing – review & editing. **Muhammad Awais:** Writing – review & editing. **Muhammad Usman:** Writing – review & editing. **Sebastien Castelltort:** Supervision, Writing – review & editing. **Thierry Adatte:** Supervision, Writing – review & editing. **Eduardo Garzanti:** Conceptualization, Supervision, Writing – original draft.

Declaration of competing interest

The authors declare that they have no known competing financial interests or personal relationships that could have appeared to influence the work reported in this paper.

Data availability

All the data are included in table 1, and in the methods and results sections

Acknowledgments

The first author is grateful to the Department of Earth and Environmental Sciences of the University of Geneva and, together with L.M., to the PhD program of the Department of Earth and Environmental Sciences of Milano Bicocca University for supporting their research. Useful critical comments by Editor in Chief Jian-Wei Li and an anonymous reviewer, as well as constructive suggestions by Sergio Andò, Or M. Bialik and Marta Barbarano are gratefully acknowledged. Open Access funding enabled and organized by the University of Geneva. This research represents a scientific contribution to Project MIUR - Dipartimenti di Eccellenza 2023-2027.

References

Abbasi, I.A., Haneef, M., Obaid, S., Daud, F., Qureshi, A.W., 2012. The Mesozoic deltaic system along the western margin of the Indian plate: lithofacies and depositional setting of Datta Formation. North Pakistan. Arabian Journal of Geosciences 5 (3), 471–480.

Afridi, A.G.K., 2010. Revalidation of Geological Map of Nathiagali Quadrangle, Abbottabad and Mansehra District, Khyber Pakhtunkhwa and Parts of Rawalpindi and Muzafarabad Districts, Pakistan Geological Survey of Pakistan; Ministry of Petroleum and Natural Research: Islamabad Pakistan. Lahore Geol Map Ser 3.

Afzal, J., Williams, M., Leng, M.J., Aldridge, R.J., Stephenson, M.H., 2011. Evolution of Paleocene to Early Eocene larger benthic foraminifer assemblages of the Indus Basin. Pakistan. Lethaia 44 (3), 299–320.

Afzal, J., Williams, M., Leng, M.J., Aldridge, R.J., 2011b. Dynamic response of the shallow marine benthic ecosystem to regional and pan-Tethyan environmental change at the Paleocene-Eocene boundary. Palaeogeogr. Palaeoclimatol. Palaeoecol. 309 (3–4), 141–160.

Aguilera, O., Bencomo, K., de Araújo, O.M.O., Dias, B.B., Coletti, G., Lima, D., Silane, A. F., Polk, M., Alves-Martin, M.V., Jaramillo, C., Kutter, V.T., Lopes, R.T., 2020. Miocene heterozoan carbonate systems from the western Atlantic equatorial margin in South America: The Pirabas formation. Sed. Geol. 407, 1–28.

Aguirre, J., Riding, R., Braga, J.C., 2000. Late Cretaceous incident light reduction: evidence from benthic algae. Lethaia 33 (3), 205–213.

Aguirre, J., Baceta, J.I., Braga, J.C., 2022. Coralline Algae at the Paleocene/Eocene Thermal Maximum in the Southern Pyrenees (N Spain). Front. Mar. Sci. 9, 899877.

Ahsan, N., 2008. Facies modeling, depositional and diagenetic environments of Kawagarh Formation, Hazara Basin, Pakistan. University of the Punjab, Lahore, Pakistan. Unpublished Ph.D. thesis.

Ahsan, N., Chaudhry, M.N., 2008. Geology of Hettangian to middle Eocene rocks of Hazara and Kashmir basins, Northwest lesser Himalayas, Pakistan. Geological Bulletin of the Punjab University 43, 131–152.

Baceta, J.I., Victoriano, P., Bernaola, G., 2005. Paleocene coralgal reefs of the western Pyrenean basin, northern Spain: New evidence supporting an earliest Paleogene recovery of reefal ecosystems. Palaeogeogr. Palaeoclimatol. Palaeoecol. 224 (1–3), 117–143.

Bagherpour, B., Vaziri, M.R., 2012. Facies, paleoenvironment, carbonate platform and facies changes across Paleocene Eocene of the Taleh Zang Formation in the Zagros Basin. SW-Iran. *Historical Biology* 24 (2), 121–142.

Banerjee, S., Choudhury, T.R., Saraswati, P.K., Khanolkar, S., 2020. The formation of authigenic deposits during Paleogene warm climatic intervals: A review. J. Palaeogeogr. 9 (1), 1–27.

Barnet, J.S.K., Littler, K., Westerhold, T., Kroon, D., Leng, M.J., Bailey, I., Röhl, U., Zachos, J.C., 2019. A high-Fidelity benthic stable isotope record of late Cretaceous–early Eocene climate change and carbon-cycling. Paleoceanogr. Paleoclimatol. 34 (4), 672–691.

Benedetti, A., Papazzoni, C.A., 2022. Rise and fall of rotaliid foraminifera across the Paleocene and Eocene times. Micropaleontology 68 (2), 185–196.

Benedetti, A., Marino, M., Pichezzi, R.M., 2018. Paleocene to Lower Eocene larger foraminiferal assemblages from Central Italy: New remarks on biostratigraphy. Riv. Ital. Paleontol. Stratigr. 124, 73–90.

Benisek, M.F., Betzler, C., Marcano, G., Mutti, M., 2009. Coralline-algal assemblages of a Burdigalian platform slope: implications for carbonate platform reconstruction (northern Sardinia, western Mediterranean Sea). Facies 55, 375–386.

Bialik, O.M., Coletti, G., Mariani, L., et al., 2023. Availability and type of energy regulate the global distribution of neritic carbonates. Sci Rep 13, 19687. https://doi.org/10.1038/s41598-023-47029-4.

Bosellini, F.R., 1998. Diversity, composition and structure of Late Eocene shelf-edge coral associations (Nago Limestone, Northern Italy). Facies 39 (1), 203–225.

Bosellini, F.R., 2006. Biotic changes and their control on Oligocene-Miocene reefs: A case study from the Apulia Platform margin (southern Italy). Palaeogeogr. Palaeoclimatol. Palaeoecol. 241 (3–4), 393–409.

Bosellini, F.R., Perrin, C., 2008. Estimating Mediterranean Oligocene-Miocene sea-surface temperatures: An approach based on coral taxonomic richness. Palaeogeogr. Palaeoclimatol. Palaeoecol. 258 (1–2), 71–88.

Bosellini, F.R., Vescogni, A., Budd, A.F., Papazzoni, C.A., 2021. High coral diversity is coupled with reef-building capacity during the Late Oligocene Warming Event (Castro Limestone, Salento Peninsula, S Italy). Riv. Ital. Paleontol. Stratigr. 127 (3), 515–538.

Bosellini, F.R., Benedetti, A., Budd, A.F., Papazzoni, C.A., 2022. A Coral Hotspot from a Hot past: The EECO and Post-EECO rich reef coral fauna from Friuli (Eocene, NE Italy), Palaeogeography, Palaeoclimatolology. Palaeoecology 607, 111284.

Bossart, P., Dietrich, D., Greco, A., Ottiger, R., Ramsay, J.G., 1988. The tectonic structure of the Hazara-Kashmir syntaxis, southern Himalayas. Pakistan. Tectonics 7 (2), 273–297.

Bowen, G.J., Maibauer, B.J., Kraus, M., Röhl, U., Westerhold, T., Steimke, A., Gingerich, P.D., Wing, S.L., Clyde, W.C., 2015. Two massive, rapid releases of carbon during the onset of the Paleocene-Eocene thermal maximum. Nat. Geosci. 8 (1), 44–47.

Butt, A.A., 1972. Problems of stratigraphic nomenclature in the Hazara District, NWFP, Pakistan. Geological Bulletin of the Punjab University 9, 65–69.

Carey, J.S., Moslow, T.F., Barrie, J.V., 1995. Origin and distribution of Holocene temperate carbonates, Hecate Strait, western Canada continental shelf. J. Sediment. Res. 65 (1a), 185–194.

Coletti, G., El Kateb, A., Basso, D., Cavallo, A., Spezzaferri, S., 2017. Nutrient influence on fossil carbonate factories: Evidence from SEDEX extractions on Burdigalian limestones (Miocene, NW Italy and S France). Palaeogeogr. Palaeoclimatol. Palaeoecol. 475, 80–92.

Coletti, G., Basso, D., Corselli, C., 2018. Coralline algae as depth indicators in the Sommières Basin (early Miocene, Southern France). Geobios 51 (1), 15–30.

Coletti, G., Basso, D., Betzler, C., Robertson, A.H., Bosio, G., El Kateb, A., Foubert, A., Meilijson, A., Spezzaferri, S., 2019. Environmental evolution and geological significance of the Miocene carbonates of the Eratosthenes Seamount (ODP Leg 160). Palaeogeogr. Palaeoclimatol. Palaeoecol. 530, 217–235.

Coletti, G., Basso, D., 2020. Coralline algae as depth indicators in the Miocene carbonates of the Eratosthenes Seamount (ODP Leg 160, Hole 966F). Geobios 60, 29–46.

Coletti, G., Balmer, E.M., Bialik, O.M., Cannings, T., Kroon, D., Robertson, A.H., Basso, D., 2021a. Microfacies evidence for the evolution of Miocene coral-reef environments in Cyprus. Palaeogeogr. Palaeoclimatol. Palaeoecol. 584, 110670.

Coletti, G., Mariani, L., Garzanti, E., Consani, S., Bosio, G., Vezzoli, G., Hu, X., Basso, D., 2021b. Skeletal assemblages and terrigenous input in the Eocene carbonate systems of the Nummulitic Limestone (NW Europe). Sed. Geol. 425, 106005.

Coletti, G., Commissario, L., Mariani, L., Bosio, G., Desbiolles, F., Soldi, M., Bialik, O.M., 2022. Palaeocene to Miocene southern Tethyan carbonate factories: A meta-analysis of the successions of South-western and Western Central Asia. The Depositional Record 8 (3), 1031–1054.

Cornacchia, I., Brandano, M., Agostini, S., 2021. Miocene paleoceanographic evolution of the Mediterranean area and carbonate production changes: A review. Earth Sci. Rev. 221, 103785.

Crabbe, M.J.C., 2008. Climate change, global warming and coral reefs: modelling the effects of temperature. Comput. Biol. Chem. 32 (5), 311–314.

Critelli, S., Garzanti, E., 1994. Provenance of the lower Tertiary Murree redbeds (Hazara-Kashmir Syntaxis, Pakistan) and initial rising of the Himalayas. Sed. Geol. 89 (3–4), 265–284.

Di Carlo, M., Accordi, G., Carbone, F., Pignatti, J., 2010. Biostratigraphic analysis of Paleogene lowstand wedge conglomerates of a tectonically active platform margin (Zakynthos Islands, Greece). Journal of Mediterranean Earth Sciences 2, 31–92.

DiPietro, J.A., Pogue, K.R., 2004. Tectonostratigraphic subdivisions of the Himalaya: A view from the west. Tectonics 23 (5), 1–20.

Dunham, R.J., 1962. In: Ham, W.E. (Ed.), Classification of carbonate rocks, 1. Memoir of American Association of Petroleum Geologists, pp. 108–121.

Embry, A.F., Klovan, J.E., 1971. A late Devonian reef tract on northeastern Banks Island. NWT. Bulletin of Canadian Petroleum Geology 19 (4), 730–781.

Esteban, M., 1996. An overview of Miocene reefs from Mediterranean areas: general trends and facies models. In: Franseen, E.K., Esteban, M., Ward, W.C., Rouchy, J.M. (Eds.), Models for Carbonate Stratigraphy, from Miocene Reef Complex of the Mediterranean Area. Society for Sedimentary Geology, Tulsa, Oklahoma, pp. 3–53.

Follows, E.J., Robertson, A.H.F., Scoffin, T.P., 1996. Tectonic control on Miocene reefs and related carbonate facies in Cyprus. In: Franseen, E.K., Esteban, M., Ward, W.C., Rouchy, J.M. (Eds.), Models for Carbonate Stratigraphy from Miocene Reef Complex of the Mediterranean Area Concepts in Sedimentology and Paleontology 5. Society for Sedimentary Geology, Tulsa Oklahoma U.S.A, pp. 295–315.

Garzanti, E., Baud, A., Mascle, G., 1987. Sedimentary record of the northward flight of India and its collision with Eurasia (Ladakh Himalaya, India). Geodin. Acta 1 (4–5), 297–312.

Gogoi, B., Deka Kalita, K., Garg, R., Borgohain, R., 2009. Foraminiferal biostratigraphy and palaeoenvironment of the Lakadong Limestone of the Mawsynram area, South Shillong Plateau, Meghalaya. J. Palaeontol. Soc. India 54 (2), 209.

Granier, B., 2012. The contribution of calcareous green algae to the production of limestones: A review. Geodiversitas 34 (1), 35–60.

Halfar, J., Godinez-Orta, L., Mutti, M., Valdez-Holguìn, J.E., Borges, J.M., 2004. Nutrient and temperature controls on modern carbonate production: An example from the Gulf of California, Mexico. Geology 32, 213–216.

Halfar, J., Mutti, M., 2005. Global dominance of coralline red-algal facies: A response to Miocene oceanographic events. Geology 33 (6), 481–484.

Hottinger, L., 2009. The Paleocene and earliest Eocene foraminiferal Family Miscellaneidae: Neither nummulitids nor rotaliids. Carnets de Géologie/Notebooks on Geology. Article 2009/6 (CG2009_A06).

Hottinger, L., 2014. Paleogene larger rotaliid foraminifera from the western and central neotethys. Springer Cham 191.

Hu, X., Garzanti, E., Wang, J., Huang, W., An, W., Webb, A., 2016. The timing of India-Asia collision onset–Facts, theories, controversies. Earth Sci. Rev. 160, 264–299.

Jauhri, A.K., Misra, P.K., Kishore, S., Singh, S.K., 2006. Larger foraminiferal and calcareous algal facies in the Lakadong Formation of the South Shillong Plateau, NE India. J. Palaeontol. Soc. India 51 (2), 51–61.

Jiang, J., Hu, X., Li, J., BouDagher-Fadel, M., Garzanti, E., 2021. Discovery of the Paleocene-Eocene Thermal Maximum in shallow-marine sediments of the Xigaze forearc basin, Tibet: A record of enhanced extreme precipitation and siliciclastic sediment flux. Palaeogeogr. Palaeoclimatol. Palaeoecol. 562, 110095.
Jiang, J., Hu, X., Garzanti, E., Li, J., BouDagher-Fadel, M.K., Sun, G., Xu, Y., 2022. Enhanced storm-induced turbiditic events during early Paleogene hyperthermals (Arabian continental margin, SW Iran). Global Planet. Change 214, 103832.
Johnson, K.G., Jackson, J.B., Budd, A.F., 2008. Caribbean reef development was independent of coral diversity over 28 million years. Science 319 (5869), 1521–1523.
Kahsnitz, M.M., Zhang, Q., Willems, H., 2016. Stratigraphic distribution of the larger benthic foraminifera Lockhartia in south Tibet (China). The Journal of Foraminiferal Research 46 (1), 34–47.
Kakar, A., Kasi, A.M., Benedetti, A., Kasi, A.K., 2022. Stratigraphy and depositional environment of a mixed siliciclastic-carbonate platform and slope succession of the Paleogene Nisai Group. Pakistan. Stratigraphy 19 (2), 95–117.
Kamran, M., Frontalini, F., Xi, D., Papazzoni, C.A., Jafarian, A., Latif, K., Jiang, T., Mirza, K., Song, H., Wan, X., 2021. Larger benthic foraminiferal response to the PETM in the Potwar Basin (Eastern NeoNeotethys, Pakistan). Palaeogeogr. Palaeoclimatol. Palaeoecol. 575, 110450.
Kato, A., Baba, M., Kawai, H., Masuda, M., 2006. Reassessment of the little-known crustose red algal genus *Polystrata* (Gigartinales), based on morphology and SSU rDNA sequences. J. Phycol. 42 (4), 922–933.
Kazmi, A.H., Rana, R.A., 1982. Tectonic map of Pakistan at a scale of 1:200,000. Geological Survey of Pakistan, Quetta.
Kiessling, W., Flügel, E., Golonka, J., 1999. Paleo reef maps: Evaluation of a comprehensive database on phanerozoic reefs. Am. Assoc. Pet. Geol. Bull. 83, 1552–1587.
Kiessling, W., Flügel, E., Golonka, J., 2002. Phanerozoic reef patterns. SEPM Special Publication, Tulsa, Oklahoma, USA. Society for Sedimentary Geology (SEPM) 775.
Latif, M.A., 1970. Explanatory notes on the Geology of South Eastern Hazara, to accompany the revised Geological Map. Wien Jb. Geol, BA, Sonderb, p. 15.
Leppig, U., 1988. Structural analysis and taxonomic revision of *Miscellanea*, Paleocene larger Foraminifera.- Eclogae Geologicae Helvetiae. Basel 81 (3), 689–721.
Leppig, U., Langer, M.R., 2015. Emendation and taxonomic revision of *Miscellanea juliettae pfenderae* and *M. juliettae villattea* with designation of the respective holotype. Micropaleontology 61, 227–230.
Li, J., Hu, X., Garzanti, E., An, W., Wang, J., 2015. Paleogene carbonate microfacies and sandstone provenance (Gamba area, South Tibet): Stratigraphic response to initial India-Asia continental collision. J. Asian Earth Sci. 104, 39–54.
Li, J., Hu, X., Garzanti, E., BouDagher-Fadel, M., 2017. Shallow-water carbonate responses to the Paleocene-Eocene thermal maximum in the Tethyan Himalaya (southern Tibet): Tectonic and climatic implications. Palaeogeogr. Palaeoclimatol. Palaeoecol. 466, 153–165.
Li, J., Hu, X., Zachos, J.C., Garzanti, E., BouDagher-Fadel, M., 2020. Sea level, biotic and carbon-isotope response to the Paleocene-Eocene thermal maximum in Tibetan Himalayan platform carbonates. Global Planet. Change 194, 103316.
Li, J., Hu, X., Garzanti, E., BouDagher-Fadel, M., 2022. Spatial heterogeneity in carbonate-platform environments and carbon isotope values across the Paleocene-Eocene thermal maximum (Neotethys Himalaya, South Tibet). Global Planet. Change 103853.
Lokier, S.W., Al Junaibi, M., 2016. The petrographic description of carbonate facies: are we all speaking the same language? Sedimentology 63 (7), 1843–1885.
Marshall, A.T., Clode, P., 2004. Calcification rate and the effect of temperature in a zooxanthellate and an azooxanthellate scleractinian reef coral. Coral Reefs 23 (2), 218224.
McInerney, F.A., Wing, S.L., 2011. The Paleocene-Eocene Thermal Maximum: A perturbation of carbon cycle, climate, and biosphere with implications for the future. Annu. Rev. Earth Planet. Sci. 39, 489–516.
Michel, J., Borgomano, J., Reijmer, J.J., 2018. Heterozoan carbonates: When, where and why? A synthesis on parameters controlling carbonate production and occurrences. Earth Sci. Rev. 182, 50–67.
Najman, Y., Pringle, M., Godin, L., Oliver, G., 2001. Dating of the oldest continental sediments from the Himalayan foreland basin. Nature 410 (6825), 194–197.
Najman, Y., Jenks, D., Godin, L., Boudagher-Fadel, M., Millar, I., Garzanti, E., Horstwood, M., Bracciali, L., 2017. The Tethyan Himalayan detrital record shows that India-Asia terminal collision occurred by 54 Ma in the Western Himalaya. Earth Planet. Sci. Lett. 459, 301–310.
Nebelsick, J.H., Rasser, M.W., Bassi, D., 2005. Facies dynamics in Eocene to Oligocene circumalpine carbonates. Facies 51 (1), 197–217.
Nicora, A., Garzanti, E., Fois, E., 1987. Evolution of the neotethys himalaya continental shelf during maastrichtian to paleocene (Zanskar, India). Rivista Italiana Paleontologia E Stratigrafia 92 (4), 439–496.
Ohba, H., Matsuda, S., Asami, R., Iryu, Y., 2017. Recent Dasycladales (Chlorophyta) in Okinawa Jima in the Central Ryukyus, southwestern Japan: Paleontological implications. Isl. Arc 26 (3), e12185.
Özcan, E., Hanif, M., Ali, N., Yücel, A.O., 2015. Early Eocene orthophragminids (Foraminifera) from the type-locality of *Discocyclina ranikotensis* Davies, 1927, Thal, NW Himalayas, Pakistan: Insights into the orthophragminid paleobiogeography. Geodin. Acta 27, 267–299.
Özcan, E., Pignatti, J., Pereira, C., Yücel, A.O., Drobne, K., Barattolo, F., Saraswati, P.K., 2018. Paleocene orthophragminids from the Lakadong Limestone, Mawmluh Quarry Section, Meghalaya (Shillong, NE India): Implications for the regional geology and paleobiogeography. J. Micropalaeontol. 37, 357–381.
Papazzoni, C.A., Ćosović, V., Briguglio, A., Drobne, K., 2017. Towards a calibrated larger foraminifera biostratigraphic zonation: celebratin 18 years of the application of Shallow Benthic Zones towards calibrated benthic zones. PALAIOS 32 (1), 1–4.
Pereira, C.D., Khanolkar, S., Banerjee, S., Özcan, E., Saraswati, P.K., 2022. Larger benthic foraminifera and microfacies of late Paleocene-early Eocene sections in Meghalaya, Northeast India. J. Foramin. Res. 52, 40–56.
Perrin, C., Bosellini, F.R., 2012. Paleobiogeography of scleractinian reef corals: changing patterns during the Oligocene-Miocene climatic transition in the Mediterranean. Earth Sci. Rev. 111 (1–2), 1–24.
Perrin, C., Kiessling, W., 2012. Latitudinal trends in Cenozoic reef patterns and their relationship to climate. In: Mutti, M., Piller, W., Betzler, C. (Eds.), Carbonate Systems during the Oligocene-Miocene Climatic Transition 42. Wiley-Blackwell. International Association of Sedimentologists Special Publications, Oxford, UK, pp. 17–34.
Pestana, E.M.D.S., Nunes, J.M.D.C., Cassano, V., Lyra, G.D.M., 2021. Taxonomic revision of the Peyssonneliales (Rhodophyta): Circumscribing the authentic Peyssonnelia clade and proposing four new genera and seven new species. J. Phycol. 57 (6), 1749–1767.
Pignatti, J., Papazzoni, C.A., 2017. Oppel zones and their heritage in current larger foraminiferal biostratigraphy. Lethaia 50, 369–380.
Pomar, L., 2001. Types of carbonate platforms: a genetic approach. Basin Res. 13 (3), 313–334.
Pomar, L., 2020. Chapter 12 - Carbonate systems. In: Scarselli, N., Chiarella, D., Bally, A. W., Adam, J., Roberts, D.G. (Eds.), Regional Geology and Tectonics. Elsevier, pp. 235–311.
Pomar, L., Baceta, J.I., Hallock, P., Mateu-Vicens, G., Basso, D., 2017. Reef building and carbonate production modes in the west-central Neotethys during the Cenozoic. Mar. Pet. Geol. 83, 261–304.
Ridgwell, A., Zeebe, R.E., 2005. The role of the global carbonate cycle in the regulation and evolution of the Earth system. Earth Planet. Sci. Lett. 234 (3–4), 299–315.
Riding, R., 2002. Structure and composition of organic reefs and carbonate mud mounds: concepts and categories. Earth Sci. Rev. 58 (1–2), 163–231.
Saboor, A., Ahmad, J., Khan, S., Latif, K., Khan, A., Haider, A.T., 2021. Foraminiferal biostratigraphy, facies, and sequence stratigraphy analysis across the K-Pg Boundary in Hazara, Lesser Himalayas (Dhudial Section). Geodiversitas 43 (18), 663–682.
Sameeni, S.J., Nazir, N., Abdul-Karim, A., Naz, H., 2009. Foraminiferal biostratigraphy and reconnaissance microfacies of Paleocene Lockhart Limestone of Jabri area, Hazara, northern Pakistan. Geological Bulletin of the Punjab University 44, 85–96.
Sarkar, S., 2018. The enigmatic palaeocene-eocene coralline *Distichoplax*: Approaching the structural complexities, ecological affinities and extinction hypotheses. Mar. Micropaleontol. 139, 72–83.
Sarkar, S., 2020. Ecostratigraphic implications of a Late Palaeocene shallow-marine benthic community from the Jaintia Hills, Meghalaya, NE India. J. Earth Syst. Sci. 129 (1), 10.
Sarkar, S., Narasimha Rao, G.M., 2018. Coralline red algae from late Palaeocene–earliest Eocene carbonates of Meghalaya, N-E India: palaeocommunity and trophic-level implications. Carbonates Evaporites 33, 767–781.
Sarkar, S., Cotton, L.J., Valdes, P.J., Schmidt, D.N., 2022. Shallow water records of the PETM: Novel insights from NE India (Eastern Neotethys). Paleoceanogr. Paleoclimatol. 37 (7) e2021PA004257.
Sarma, A., Ghosh, A.K., 2006. A new record of calcareous algae from shella Formation (Jaintia Group) of South Jaintia Hills, Meghalaya India. Curr. Sci. 1276–1281.
Scheibner, C., Speijer, R.P., Marzouk, A.M., 2005. Turnover of larger foraminifera during the Paleocene-Eocene Thermal Maximum and paleoclimatic control on the evolution of platform ecosystems. Geology 33 (6), 493–496.
Scheibner, C., Speijer, R.P., 2008. Late paleocene–early eocene tethyan carbonate platform evolution - A response to long-and short-term paleoclimatic change. Earth Sci. Rev. 90 (3–4), 71–102.
Serra-Kiel, J., Hottinger, L., Caus, E., Drobne, K., Ferrandez, C., Jauhri, A.K., Less, G., Pavlovec, R., Pignatti, J., Samso, J.M., Schaub, H., Sirel, E., Strougo, A., Tambareau, Y., Tosquella, J., Zakrevskaya, E., 1998. Larger foraminiferal biostratigraphy of the Tethyan. Bulletin De La Société Géologique De France 169, 281–299.
Serra-Kiel, J., Vicedo, V., Baceta, J.I., Bernaola, G., Robador, A., 2020. Paleocene Larger Foraminifera from the Pyrenean Basin with a recalibration of the Paleocene Shallow Benthic Zones. Geol. Acta 18, 1–69. I-III.
Shah, M.M., Rahim, H.U., Hassan, A., Mustafa, M.R., Ahmad, I., 2020. Facies control on selective dolomitization and its impact on reservoir heterogeneities in the Samana Suk Formation (Middle Jurassic), Southern Hazara Basin (NW Himalaya, Pakistan): An outcrop analogue. Geosci. J. 24 (3), 295–314.
Shah, S.M.I., 2009. Stratigraphy of Pakistan. Memoirs of the Geological Survey of Pakistan, 22.
Shalalvand, M., Adabi, M., Zohdi, A., 2021. Biological evolution of the carbonate platform of the Taleh Zang Formation in Kermanshah region. Journal of Stratigraphy and Sedimentology Researches 37 (1), 45–66.
Sirel, E., 2018. Revision of the paleocene and partly early eocene larger benthic foraminifera of Turkey. Department of Geological Engineering Ankara University: Ankara Üniversitesi Yayýnevi Yayin 27, 260.
Stanley, S.M., Hardie, L.A., 1998. Secular oscillations in the carbonate mineralogy of reef-building and sediment-producing organisms driven by tectonically forced shifts in seawater chemistry. Palaeogeogr. Palaeoclimatol. Palaeoecol. 144 (1–2), 3–19.
Sternai, P., Caricchi, L., Pasquero, C., Garzanti, E., van Hinsbergen, D.J., Castelltort, S., 2020. Magmatic forcing of Cenozoic climate? Journal of Geophysical Research: Solid Earth 125 (1) e2018JB016460.

Titelboim, D., Almogi-Labin, A., Herut, B., Kucera, M., Asckenazi- Polivoda, S., Abramovich, S., 2019. Thermal tolerance and range expansion of invasive foraminifera under climate changes. Sci. Rep. 9 (1), 1–5.

Tremblin, M., Khozyem, H., Adatte, T., Spangenberg, J.E., Fillon, C., Grauls, A., Hunger, T., Nowak, A., Läuchli, C., Lasseur, E., Roig, J.Y., Serrano, O., Calassou, S., Guillocheau, F., Castelltort, S., 2022. Mercury enrichments of the Pyrenean foreland basins sediments support enhanced volcanism during the Paleocene-Eocene thermal maximum (PETM). Global Planet. Change 212, 103794.

Umar, M., Sabir, M.A., Farooq, M., Khan, M.M.S.S., Faridullah, F., Jadoon, U.K., Khan, A. S., 2015. Stratigraphic and sedimentological attributes in Hazara Basin Lesser Himalaya, North Pakistan: Their role in deciphering minerals potential. Arab. J. Geosci. 8 (3), 1653–1667.

Van der Zwaan, G.J., Jorissen, F.J., De Stigter, H.C., 1990. The depth dependency of planktic/benthic foraminiferal ratios: Constraints and applications. Mar. Geol. 95 (1), 1–16.

Vescogni, A., Bosellini, F.R., Reuter, M., Brachert, T.C., 2008. Vermetid reefs and their use as palaeobathymetric markers: New insights from the late miocene of the mediterranean (Southern Italy, Crete). Palaeogeogr. Palaeoclimatol. Palaeoecol. 267 (1–2), 89–101.

Vescogni, A., Bosellini, F.R., Papazzoni, C.A., Giusberti, L., Roghi, G., Fornaciari, E., Dominici, S., Zorzin, R., 2016. Coralgal buildups associated with the Bolca Fossil-Lagerstätten: New evidence from the Ypresian of Monte Postale (NE Italy). Facies 62 (3), 1–20.

Vimpere, L., Spangenberg, J., Roige, M., Adatte, T., De Kaenel, E., Fildani, A., Clark, J., Sahoo, S., Bowman, A., Sternai, P., Castelltort, S., 2023. Carbon isotope and biostratigraphic evidence for an expanded PETM sedimentary record in the deep Gulf of Mexico. Geology, 51 334–339. https://doi.org/10.1130/G50641.1.

Vršič, A., Gawlick, H.J., Schlagintweit, F., Machaniec, E., Gharsalla, M., 2021. Age, microfacies and depositional environment of the middle to late paleocene shallow-marine carbonates in the sirt basin of libya (Upper Sabil Formation): "Are Intisar domal structures pinnacle reefs?". Facies 67, 27.

Westerhold, T., Marwan, N., Drury, A.J., Liebrand, D., Agnini, C., Anagnostou, E., Barnet, J.S.K., Bohaty, S.M., De Vleeschouwer, D., Florindo, F., Frederichs, T., Hodell, D.A., Holbourn, A.E., Kroon, D., Lauretano, V., Littler, K., Lourens, L.J., Lyle, M., Pälike, H., Röhl, U., Tian, J., Wilkens, R.H., Wilson, P.A., Zachos, J.C., 2020. An astronomically dated record of Earth's climate and its predictability over the last 66 million years. Science (new York, N.Y.) 369 (6509), 1383–1387.

Wilson, M.E., 2008. Global and regional influences on equatorial shallow-marine carbonates during the Cenozoic. Palaeogeogr. Palaeoclimatol. Palaeoecol. 265 (3–4), 262–274.

Zachos, J.C., Dickens, G.R., Zeebe, R.E., 2008. An early Cenozoic perspective on greenhouse warming and carbon-cycle dynamics. Nature 451 (7176), 279–283.

Zamagni, J., Mutti, M., Košir, A., 2008. Evolution of shallow benthic communities during the Late Paleocene–earliest Eocene transition in the Northern Neotethys (SW Slovenia). Facies 54 (1), 25–43.

Zamagni, J., Mutti, M., Košir, A., 2012. The evolution of mid Paleocene-early Eocene coral communities: How to survive during rapid global warming. Palaeogeography, Alaeoclimatology, Palaeoecology 317, 48–65.

Zhang, Q., Willems, H., Ding, L., 2013. Evolution of the paleocene-early eocene larger benthic foraminifera in the tethyan himalaya of tibet, China. Int. J. Earth Sci. 102, 1427–1445.

Zhang, Q., Willems, H., Ding, L., Xu, X., 2019. Response of larger benthic foraminifera to the Paleocene-Eocene thermal maximum and the position of the Paleocene/Eocene boundary in the Tethyan shallow benthic zones: Evidence from south Tibet. GSA Bull. 131 (1–2), 84–98.